

Diastereoselective formation of calcium and ytterbium *ansa*-metallocenes via recombination of guaiazulene (Gaz) radical anions. Molecular structure of *ansa*-(η^5 -Gaz)₂Ca(THF)₂ and *ansa*-(η^5 -Gaz)₂Yb(Py)₂ (Gaz = 1,4-dimethyl-7-isopropylazulene) complexes

I. L. Fedushkin,^{a*} Yu. A. Kurskii,^a T. V. Balashova,^a M. N. Bochkarev,^a S. Dechert,^b S. Mühle,^b and H. Schumann^b

^aG. A. Razuvayev Institute of Organometallic Chemistry, Russian Academy of Sciences,
49 ul. Tropinina, 603950 Nizhnii Novgorod, Russian Federation.

Fax: +7 (831 2) 66 1497. E-mail: igorfed@imoc.snn.ru

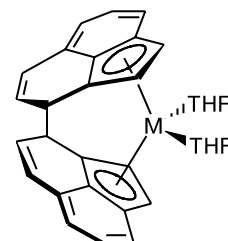
^bInstitute of Chemistry, Technical University of Berlin,
135 str. 17 June, D-10623 Berlin, Germany.*
Fax: +49 (30) 3142 2168

ansa-Metallocene derivative (η^5 -Gaz)₂Ca(THF)₂ (**1**) (Gaz = 1,4-dimethyl-7-isopropylazulene) was synthesized by the reaction of CaI₂(THF)₂ with two equivalents of potassium and two equivalents of guaiazulene in THF. The ytterbium analog *ansa*-(η^5 -Gaz)₂Yb(THF)₂ (**2a**) was synthesized by the reduction of guaiazulene with ytterbium naphthalenide in THF. The recrystallization of **2a** from pyridine leads to the exchange of the coordinated solvent molecules and gives *ansa*-(η^5 -Gaz)₂Yb(NC₅H₅)₂ (**2b**). The molecular structures of **1**, **2a**, and **2b** were determined by X-ray diffraction analysis. The crystals of **1**, **2a**, and **2c** consist of a racemic mixture of both *R,R*- and *S,S*-enantiomers. The calcium and ytterbium atoms η^5 -coordinate the five-membered rings of the guaiazulene ligands. The ¹H NMR spectroscopic and X-ray diffraction data unambiguously confirm the exclusive formation of *C*₂-symmetric *ansa*-metallocenes in these reactions. The reaction of compound **1** with Me₃SiCl in THF occurs with retention of the C–C bond between two guaiazulene moieties and affords bis(1,4-dimethyl-3-trimethylsilyl-7-isopropylazulene) (**3**) in high yield.

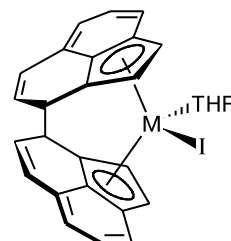
Key words: calcium, ytterbium(II), *ansa*-metallocenes, guaiazulene.

We have recently reported the stereoselective formation of lanthanide and calcium *ansa*-metallocenes ($\eta^5:\eta^5$ -C₂₄H₁₆)M(THF)₂ (M = Sm,¹ Yb,¹ Ca²) by the reduction of acenaphthylene with the corresponding metals or their naphthalenides [C₁₀H₈]²⁻M(THF)₂, or by exchange reactions of the corresponding diiodides MI₂(THF)₂ with potassium acenaphthyleneide.³ We have established¹ the molecular structures of the samarium and ytterbium derivatives by X-ray diffraction analysis. The structure of the calcium complex, which is similar to those of the Sm and Yb complexes, was determined using X-ray diffraction analysis by other authors.⁴ Acenaphthylene *ansa*-metallocenes of trivalent lanthanides ($\eta^5:\eta^5$ -C₂₄H₁₆)LnI(THF) (Ln = Dy, Er, Tm, Lu)³ were also synthesized by the reaction of lanthanide triiodides with potassium acenaphthyleneide [C₁₂H₈]⁻K⁺.

In the case of thulium, the acenaphthylene metallocene derivative ($\eta^5:\eta^5$ -C₂₄H₁₆)TmI(THF)⁵ is formed, in addition, by the treatment of acenaphthylene with thulium



M = Sm, Yb, Ca



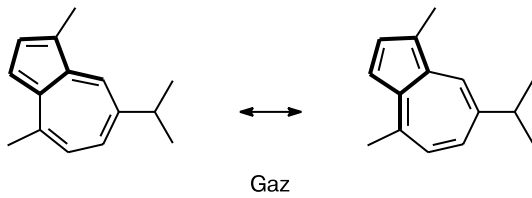
M = Dy, Er, Tm, Lu

diiodide. In all chemical reactions listed above, the acenaphthylene radical anions are dimerized only selectively and give rise to racemic *C*₂-symmetric *ansa*-metallocenes. The recombination of the acenaphthylene radical anions discovered by us can be attributed to the reductive dimerization of different 6-mono- and 6,6'-disubstituted pentafulvalenes.⁶ Note, however, that both *rac*- and *meso*-isomers of *ansa*-metallocenes are formed when 6-monosubstituted pentafulvalenes (for example, 6-phenylfulvalene)^{6d} or 6,6'-disubstituted indenylidenes (for example, 6,6'-dimethylbenzofulvene)^{6e} are used.

* Institut für Chemie der Technischen Universität Berlin, Straße des 17. Juni 135, D-10623 Berlin, Germany.

1,4-Dimethyl-7-isopropylazulene (Gaz) is a non-alternant, commercially available, polycyclic hydrocarbon, whose resonance structures, as in acenaphthylene, contain the fulvene moiety (Scheme 1). Several different transition metal complexes with azulene (Az) and guaiazulene have been synthesized to the present time: $(\mu_2\text{-}\eta^3\text{-}\eta^5\text{-Gaz})\text{Fe}_2(\text{CO})_5$,⁷ $(\mu_2\text{-}\eta^5\text{-}\eta^4\text{-Az})_2\text{Fe}_4(\text{CO})_{10}$,⁸ $(\eta^5\text{-Az})_2\text{Mn}_2(\text{CO})_6$,⁹ $(\eta^5\text{-Gaz})\text{Ru}(\text{CO})_2\text{Cl}$,¹⁰ and $(\eta^6\text{-Az})\text{Mo}(\eta^6\text{-C}_6\text{H}_6)$.¹¹ These compounds are formed in low yields on refluxing of transition metal carbonyls with azulene or guaiazulene in hexane or heptane. Azulene dimerization was observed when iron⁸ and manganese⁹ carbonyls were introduced. The dimerization of guaiazulene has been reported¹² by the treatment with magnesium in THF in the presence of CH_2Cl_2 . This reaction afforded a magnesium derivative in 31% yield only and, according to the authors' opinion, it is an *exo*-complex with two MgCl moieties coordinating the five-membered rings of the diguaiazulene dianion: $(\text{Gaz})_2(\text{MgCl})_2$. The *rac*-*ansa*-(Gaz)₂TiCl₂ compound was synthesized in 10% yield by the reaction of $\text{TiCl}_3(\text{THF})_3$ with the magnesium derivative indicated. The *rac*-*ansa*-(Gaz)₂TiCl₂ complex was characterized by X-ray diffraction analysis and ¹H NMR spectroscopy.¹² It remained unclear¹² whether the formation of the *rac*-*ansa*-metallocene structure is related to the transfer of the diguaiazulene ligand from magnesium to titanium with retention of the dimerized guaiazulene configuration or it is a result of the separation of other isomers during the isolation of the *rac*-*ansa*-(Gaz)₂TiCl₂ complex.

Scheme 1

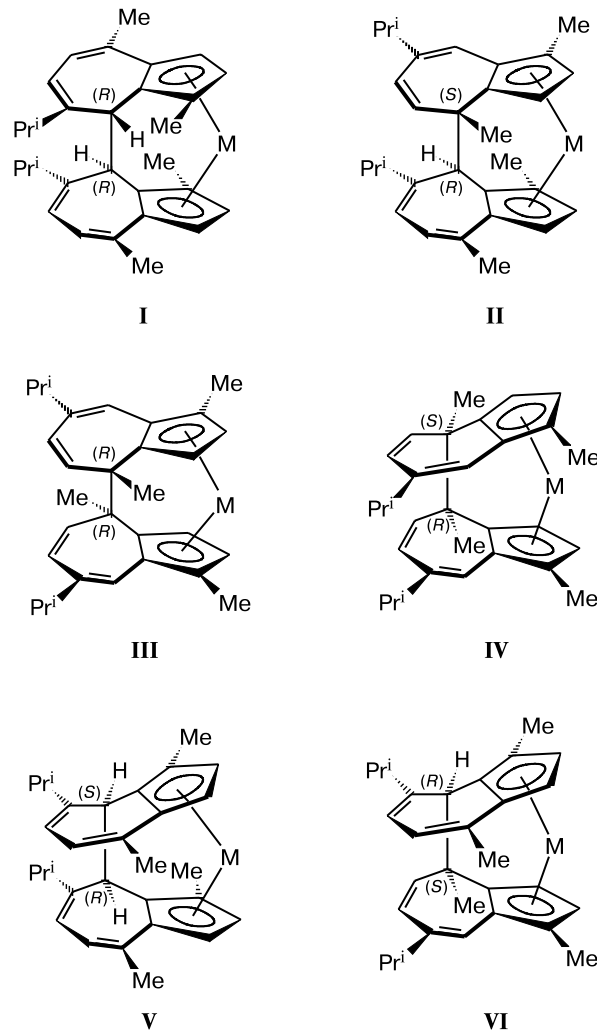


Continuing the studies of the stereoselective syntheses of lanthanide and calcium *ansa*-metallocenes using nonalternant hydrocarbons as ligands, we studied the possibility to synthesize calcium and lanthanide *ansa*-metallocenes through the reductive dimerization of 1,4-dimethyl-7-isopropylazulene (guaiazulene). In this work, we report the synthesis, structure, and some properties of the calcium and ytterbium *ansa*-metallocene guaiazulene complexes.

Results and Discussion

Radical anions of unsubstituted azulene can theoretically recombine equiprobably at two positions adjacent to

the five-membered ring with the formation of *rac*- or *meso*-*ansa*-metallocenes. In the case where these positions are nonequivalent (for example, in guaiazulene), the recombination of its radical anions on metal cations can occur to form six different diastereomeric *ansa*-metallocenes (**I**–**VI**).



Synthesis of *ansa*-($\eta^5\text{-Gaz}$)₂M(THF)₂ (M = Ca, Yb).

In order to obtain the calcium guaiazulene *ansa*-metallocene derivative, a suspension of CaI_2 was stirred in THF in the presence of potassium metal (2 equiv.) and guaiazulene (2 equiv.). It was found that the target product can be isolated in the individual state only under specific conditions of synthesis. For example, stirring of the reactants (CaI_2 , K, Gaz) in THF at ~ 20 °C produces a mixture of unidentified products after the complete dissolution of potassium and disappearance of the intense blue color of guaiazulene. Only when the reaction is carried out at 60 °C for 4.5 h with vigorous stirring followed by keeping of the reaction mixture for 3 days at ~ 20 °C, the target *ansa*-($\eta^5\text{-Gaz}$)₂Ca(THF)₂ complex (**1**) was obtained. It was isolated by recrystallization from THF in 66% yield

as colorless crystals. The ¹H NMR spectrum of the reaction mixture shows that only one isomer of *ansa*-calcoocene (isomer **1**) is formed under these conditions. Perhaps, when the reaction is carried out at ~20 °C, the radical anions that formed slowly react with CaI₂, whose solubility in THF at 20 °C is not high. As a result, the guaiazulene radical anion can further be reduced to the dianion. The subsequent protonation of this dianion (with guaiazulene or a solvent) gives rise to a mixture of products, which can contain the guaiazulene radical anion ([GazH][−]) and the products of proton elimination from the Me group of guaiazulene or THF molecule with ethylene elimination resulting in enolate CH₂=CH—OK. The latter hypothesis can be confirmed by the formation of unidentified gaseous products and the appearance of additional signals of protons (a doublet at δ 4.86 and a signal closed by a doublet of the complex at δ 5.62; the ratio of the integral intensities of these signals is 2 : 1) in the ¹H NMR spectrum of the reaction mixture along with the signals from protons of complex **1**. It should be mentioned that the protonation of dimethylfulvalene during its reduction and formation of bis(isopropylcyclopentadienyl)metallocenes has already been reported previously.¹³ Compound **1** is moderately soluble in THF and poorly soluble in Et₂O and toluene. Guaiazulene is isolated when the complex is oxidized by air oxygen. Only one set of signals of protons of the azulene ligand is manifested in the ¹H NMR spec-

trum of compound **1** recrystallized from THF (Fig. 1), which indicates the formation of only one isomer. The integration of signals of the ligand and THF molecules shows that the calcium atom in the complex coordinates two solvent molecules. An interesting feature of the ¹H NMR spectrum of complex **1** is the presence of two different signals of the Me groups of the isopropyl substituent (see Fig. 1, doublets 9 and 10). Magnetic non-equivalence of the Me groups at the prochiral center appears due to diastereotopism because of the planar chirality of the ligand. The diastereotopic splitting values of protons of the Me groups in complexes **1** in THF and **2** in Py are equal to 54 and 16 Hz, respectively. All signals in the spectrum of the calcium complex were assigned, as shown in Fig. 1, using correlation ¹H—¹H COSY NMR spectroscopy.

The procedure used for the synthesis of the calcium complex does not allow one to obtain the ytterbium analog of complex **1** in the case of YbI₂. When stirring a mixture of YbI₂, guaiazulene (2 equiv.), and potassium (2 equiv.) in THF or MeO(CH₂)₂OMe, a purple or green color of the reaction mixture appears at the initial stages (during several minutes), which is characteristic of ytterbium(II) biscyclopentadienides in THF and MeO(CH₂)₂OMe, respectively. However, the mixture discolors rapidly to form a plentiful insoluble weakly colored precipitate, which was not identified. The ytterbium com-

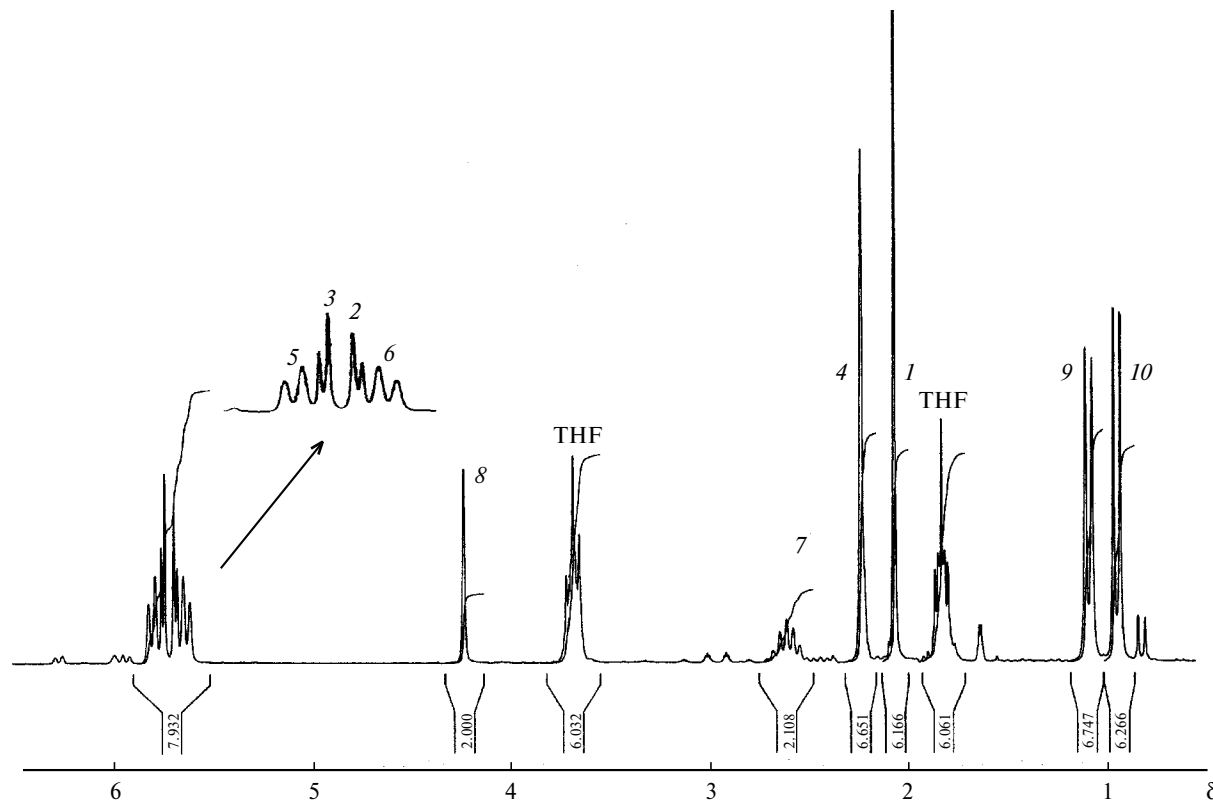


Fig. 1. ¹H NMR spectrum of complex **1** (200 MHz, THF-d₈).

plex *ansa*-(η^5 -Gaz)₂Yb(THF)₂ was obtained by the reduction of guaiazulene with ytterbium naphthalenide C₁₀H₈Yb(THF)₂ in THF. Mixing of guaiazulene and C₁₀H₈Yb(THF)₂ in THF results in the instant dissolution of a suspension of the naphthalene complex, the blue color disappears, and a red-brown solution is formed. As in the case of the calcium derivative, an attempt to isolate the reaction product immediately after the transformation of the starting reactants was unsuccessful. So, the removal of the solvent from the reaction mixture produces a viscous oily residue. The target product is crystallized during several days from a concentrated solution in THF as red lamellar crystals of *ansa*-(η^5 -Gaz)₂Yb(THF)₂ (**2a**). Recrystallization of **2a** from Py gives *ansa*-(η^5 -Gaz)₂Yb(NC₅H₅)₂ (**2b**) as black prismatic crystals. Compounds **1**, **2a**, and **2b** are poorly soluble in toluene and insoluble in hexane and Et₂O. The ¹H NMR spectra of complex **2a** in benzene or Py exhibit the same set of signals of protons of the guaiazulene ligand as that of the calcium complex.

Molecular structures of complexes **1, **2a**, and **2b**.** X-ray diffraction analysis of complexes **1**, **2a**, and **2b** shows that the dimerization of two guaiazulene radical anions and their coordination on the Ca or Yb atoms result in the formation of the *rac*-*ansa*-metallocene complexes. The crystallographic data, parameters of X-ray diffraction analysis, and refinement parameters for complexes **1**, **2a**, and **2b** are presented in Table 1. The main bond lengths in complexes **1**, **2a**, and **2b** are presented in Table 2. The unit cell of the crystal of complex **1** contains four enantiomeric pairs of molecules, whereas the unit cells of complexes **2a** and **2b** contain two pairs of enantiomeric molecules. The crystals of complexes **1**, **2a**, and **2b** are center-symmetric and contain a racemic mixture of *R,R*- and *S,S*-enantiomers. The molecular structures of complexes **1** (*R,R*-enantiomer) and **2b** (*S,S*-enantiomer) are presented in Figs. 2 and 3, respectively. The structure of complex **2a** is almost the same as that of complex **1** and, hence, the latter is not presented in the figure. The atom numbering scheme in complex **2a** given in Table 2 corresponds to the

Table 1. Crystallographic data, parameters of X-ray diffraction experiments, and refinement parameters for structures **1**, **2a**, and **2b**

Parameter	1	2a	2b
Molecular formula	C ₃₈ H ₅₂ CaO ₂	C ₃₈ H ₅₂ O ₂ Yb • C ₄ H ₈ O	C ₄₀ H ₄₆ N ₂ Yb • C ₅ H ₅ N
Molecular weight	580.88	785.94	806.93
Wavelength/Å	0.71073	0.71073	0.71073
Crystal system	Orthorhombic	Monoclinic	Monoclinic
Space group	<i>Iba</i> 2	<i>P</i> 2 ₁ /c	<i>P</i> 2 ₁ /n
Unit cell parameters			
<i>a</i> /Å	25.9376(1)	15.2603(2)	9.7392(1)
<i>b</i> /Å	15.5372(2)	17.4541(3)	15.6890(2)
<i>c</i> /Å	16.8812(1)	14.2293(1)	24.7021(1)
β /deg	90	96.50	92.60
<i>V</i> /Å ³	6803.08(10)	3765.69(9)	3770.54(6)
<i>Z</i>	8	4	4
ρ_{calc} /g cm ⁻³	1.134	1.386	1.421
μ /mm ⁻¹	0.215	2.519	2.515
<i>F</i> (000)	2528	1624	1648
Size of crystal/mm ³	0.44×0.38×0.10	0.46×0.26×0.06	0.30×0.18×0.14
Region of measurements, θ /deg	1.53—25.00	1.34—27.5	1.54—27.50
Number of observed /independent reflections	16680/5457 ($R_{\text{int}} = 0.1169$)	28243/8650 ($R_{\text{int}} = 0.0700$)	28094/8654 ($R_{\text{int}} = 0.0778$)
Completeness of data collection (%)	99.8	99.9	100.0
Number of refined parameters	5457/1/375	8650/11/415	8654/0/493
GOOF (F^2)	1.002	1.002	1.068
R_1 / wR_2 ($I > 2\sigma(I)$)	0.0698/0.1129	0.0423/0.0968	0.0453/0.0742
R_1 / wR_2 (against all parameters)	0.1384/0.1329	0.0681/0.1076	0.0786/0.0829
Residual electron density (e·Å ⁻³), $\rho_{\text{max}}/\rho_{\text{min}}$	0.247/−0.388	1.374/−2.328	1.158/−1.115

Table 2. Main bond lengths (d/Å) in complexes **1**, **2a**, and **2b**

Bond	1	2a	2b
M—O(1)	2.414(4)	2.419(3)	—
M—O(2)	2.321(4)	2.405(4)	—
M—N(1)	—	—	2.561(4)
M—N(2)	—	—	2.561(4)
M—C(1)	2.690(5)	2.695(4)	2.722(5)
M—C(2)	2.653(5)	2.683(4)	2.701(5)
M—C(3)	2.662(5)	2.683(5)	2.712(4)
M—C(4)	2.733(6)	2.702(5)	2.716(4)
M—C(5)	2.762(5)	2.744(4)	2.739(5)
M—C(16)	2.705(5)	2.680(4)	2.725(4)
M—C(17)	2.696(5)	2.683(4)	2.718(4)
M—C(18)	2.666(6)	2.694(5)	2.722(4)
M—C(19)	2.664(6)	2.687(5)	2.727(4)
M—C(20)	2.731(6)	2.707(5)	2.752(4)

numbering indicated in Fig. 2 for complex **1**. The Ca and Yb atoms in complexes **1**, **2a**, and **2b** η^5 -coordinate two five-membered rings of the guaiazulene ligands. The coordination spheres of the metal atoms in complexes **1** and **2a** also contain two THF molecules, whereas in complex **2b** the Yb atom coordinates two Py molecules. The O and N atoms of the coordinatively bound Py and THF molecules lie virtually in the bisector plane of the $C_{\text{pentr}}\text{—M—}C_{\text{pentr}}$ angle (C_{pentr} is the center of the five-membered ring). Thus, the metal atoms in complexes **1**, **2a**, and **2b** exhibit the distorted tetrahedral coordination. Since the ion radii for Ca^{II} and Yb^{II} are close, no significant differences are observed in the molecular geometry of complexes **1**, **2a**, and **2b**. The distances from

the Ca atom to the C atoms of the five-membered rings of the guaiazulene moieties and to the O atoms of the THF molecules (see Table 2) lie in the interval of bond lengths found for other calcium *ansa*-metallocene complexes: $\text{Me}_4\text{C}_2(\eta^5\text{—C}_5\text{H}_4)_2\text{Ca}(\text{Bu}^t\text{N}(\text{CH})_2\text{N}(\text{Bu}^t)_2$,^{6b} *cis*- and *trans*- $\text{Ph}_2\text{C}_2\text{H}_2(\eta^5\text{—C}_5\text{H}_4)_2\text{Ca}(\text{THF})_2$,^{6c,14} *trans*- $\text{Ph}_2\text{C}_2\text{H}_2\text{-}rac\text{-}(\eta^5\text{—4,7-Me}_2\text{C}_9\text{H}_4)_2\text{Ca}(\text{THF})_2$,^{6d} *trans*- $\text{Ph}_2\text{Me}_2\text{C}_2(\eta^5\text{—C}_5\text{H}_4)_2\text{Ca}(\text{DME})$,¹⁵ *rac*- $(\eta^5\text{—C}_24\text{H}_16)_2\text{Ca}(\text{THF})_2$,¹⁶ *meso*- $[1,1\text{'}\text{—}(1,2\text{-Bu}^t)_2\text{C}_2\text{H}_2](\eta^5\text{—C}_5\text{H}_4)_2\text{Ca}(\text{DME})$,¹⁷ and *rac*- $[1,1\text{'}\text{—}(1,2\text{-Bu}^t)_2\text{C}_2\text{H}_2](\eta^5\text{—C}_5\text{H}_4)_2\text{Ca}(\text{DME})$.¹⁷ The bonding distances from the ytterbium atoms to the five-membered rings of the guaiazulene ligand and coordinated solvent molecules are close to the corresponding values in other ytterbium *ansa*-metallocene complexes: *rac*- $(\eta^5\text{—C}_24\text{H}_16)_2\text{Yb}(\text{THF})_2$ (2.72 Å),¹ *meso*- $[(\eta^5\text{—C}_9\text{H}_6)_2(\text{CH}_2)_2\text{-}1]\text{Yb}(\text{THF})_2$ (122.0°),¹⁸ *rac*- $[(\eta^5\text{—C}_9\text{H}_6)_2(\text{CH}_2)_2\text{-}1]\text{Yb}(\text{THF})_2$ and *rac*- $[(\eta^5\text{—C}_9\text{H}_6\text{Me}_2\text{-4,7})_2(\text{CH}_2)_2\text{-}1]\text{Yb}(\text{THF})_2$.¹⁹ In complexes **1**, **2a**, and **2b**, the C—C bonds in the five-membered ring are equalized, while the seven-membered rings exhibit the pronounced alternation of the double and ordinary carbon—carbon bonds (see Table 2). The distribution of lengths of the framework C—C bonds in the guaiazulene moieties in complex **1** is presented in Fig. 4.

Reaction of complex **1 with Me_3SiCl .** We have previously shown^{2,3} that the reaction of the calcium acenaphthylene complex *ansa*- $(\eta^5\text{—C}_24\text{H}_16)_2\text{Ca}(\text{THF})_2$ (synthesized by the reduction of acenaphthylene with calcium metal or its naphthalenide) with Me_3SiCl in THF occurs with the cleavage of the bond between two cyclopentadienyl moieties to afford 1,2-bis(trimethylsilyl)ace-

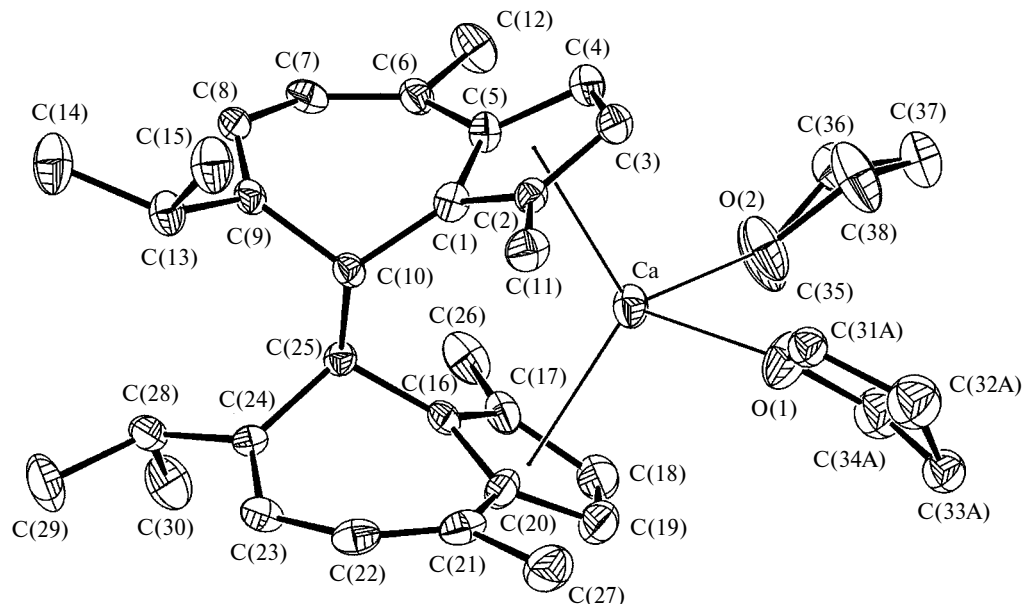


Fig. 2. Molecular structure (ORTEP image) of the $(\eta^5\text{—C}_15\text{H}_18)_2\text{Ca}(\text{THF})_2$ complex (**1**) (*R,R*-enantiomer). Thermal ellipsoids are presented (50%). Hydrogen atoms are not shown.

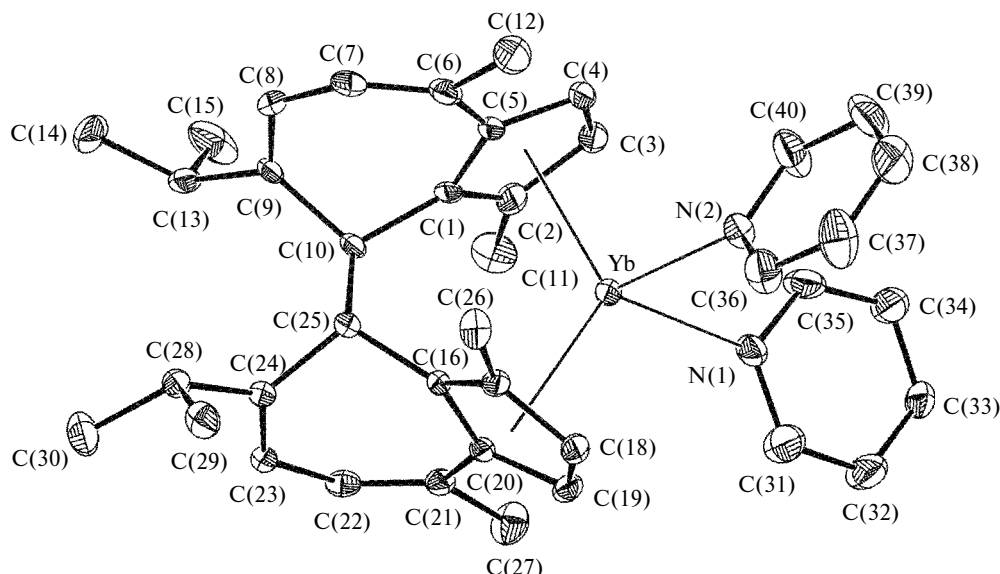


Fig. 3. Molecular structure (ORTEP image) of the $(\eta^5\text{-C}_{15}\text{H}_{18})_2\text{Yb}(\text{NC}_5\text{H}_5)_2$ (**2b**) (*S,S*-enantiomer). Thermal ellipsoids are presented (50%). Hydrogen atoms are not shown.

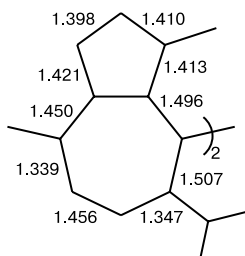
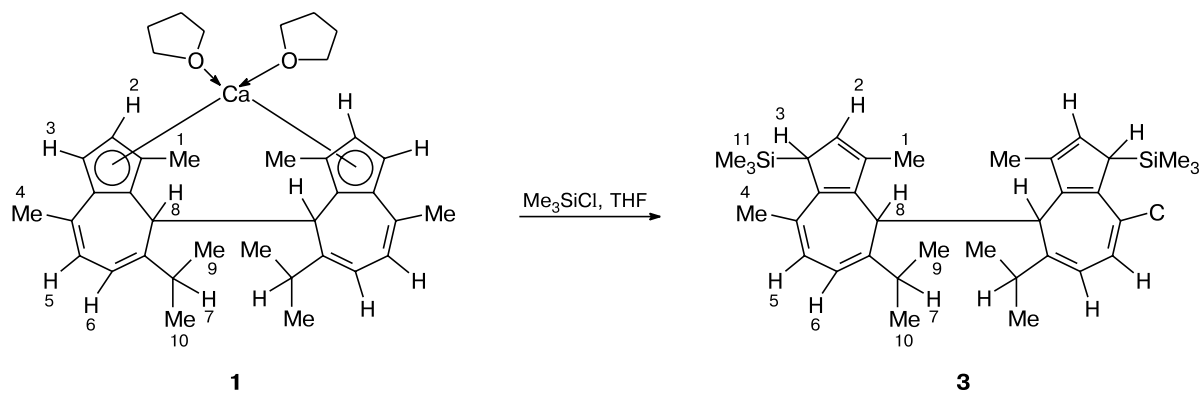


Fig. 4. Distribution of the carbon–carbon bond lengths (Å) in the guaiazulene moiety of complex **1** (average for both *Gaz* moieties).

naphthalene and free acenaphthylene in ~100% yields. Taking into account that both acenaphthylene and guaiazulene are nonalternant hydrocarbons and the radical anions formed upon their reduction are dimerized to produce *ansa*-metallocenes, we assumed that the reactions of

quaiazulene derivatives occur similarly to the reactions of the acenaphthylene complexes. Unexpectedly it turned out that the reaction of the *ansa*-($\eta^5\text{-Gaz}$)₂Ca(THF)₂ complex (**1**) with Me_3SiCl , unlike the acenaphthylene complexes, does not lead to the cleavage of the carbon–carbon bond between the cene ligands but produces bis(trimethylsilyl)diguaiazulene, $[\text{Gaz}(\text{TMS})_2]$ (**3**) (Scheme 2). The data of the ¹H NMR and correlation ¹H–¹H COSY NMR spectra (Fig. 5) indicate that the trimethylsilyl group is added to position 3 of guaiazulene. The protons of the Me(1) and Me(4) groups appear in the spectrum as singlets as δ 1.52 and 2.15, respectively. The singlet at δ 5.96 corresponding to H(2) has a cross-peak with the resonance of the Me(1) group and the resonance of the methine H(3) proton (a septet at δ 3.44). Two doublets at δ 6.19 and 5.69 (the H(5) and H(6) protons, respectively) have cross-peaks with the signals of the Me(4) group (δ 2.15). The doublet of H(6) also exhibits

Scheme 2



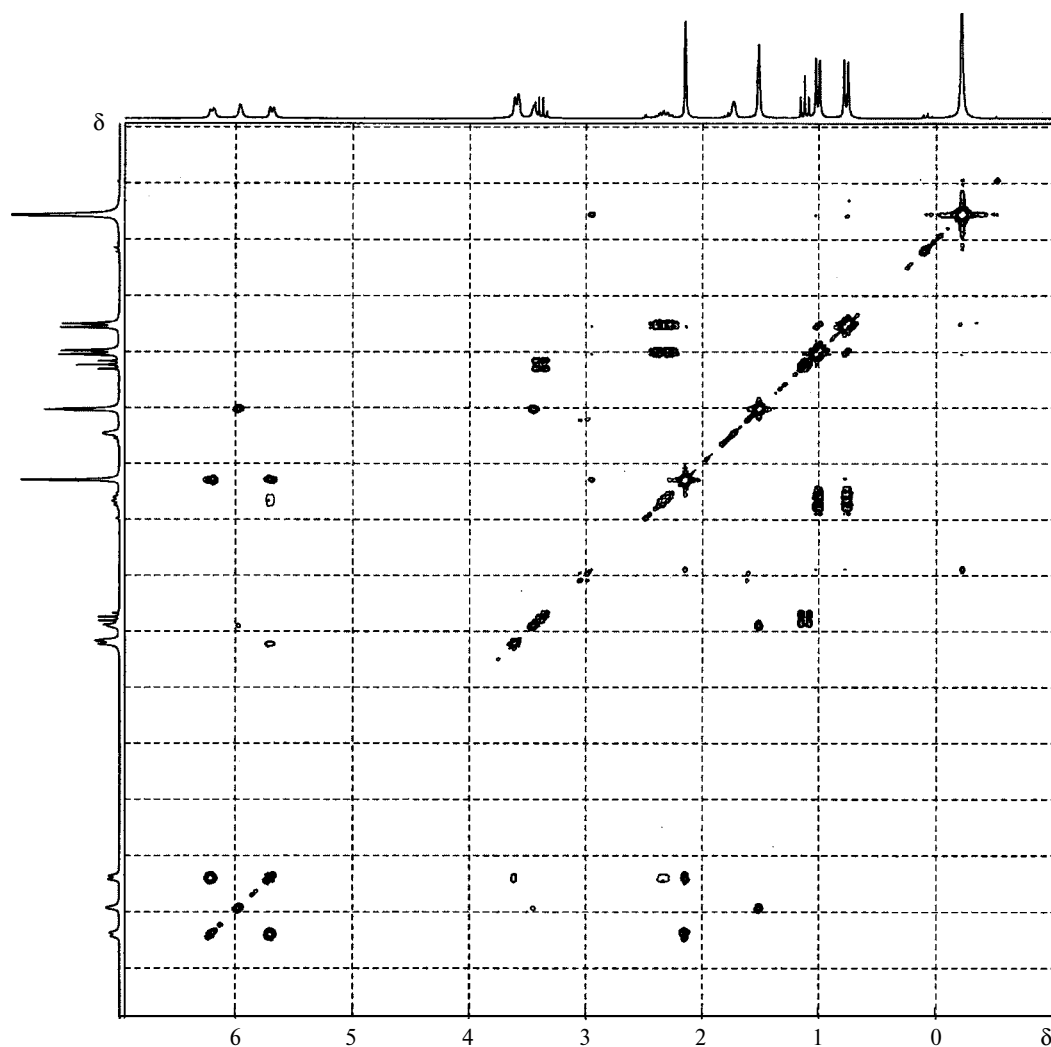


Fig. 5. Correlation ^1H — ^1H COSY NMR spectrum of compound 3 (200 MHz, C_6D_6).

cross-peaks with the signals of the methine H(8) (multiplet, δ 2.33) and H(10) protons (singlet, δ 3.61).

In our opinion, different directions of the reactions of the acenaphthylene and guaiazulene calcium *ansa*-metallocene complexes with Me_3SiCl are related to the difference in the first and second reduction potentials of acenaphthylene and guaiazulene. The first reduction potentials of both hydrocarbons differ insignificantly ($E^\circ = -1.63$ and -1.65 V for acenaphthylene and guaiazulene, respectively, in THF vs. saturated calomel electrode),²⁰ while the second reduction potential of guaiazulene is much more negative ($E^\circ = -2.45$ V)²⁰ than the second reduction potential of acenaphthylene ($E^\circ = -1.85$ V).²⁰ Unlike the acenaphthylene complexes in a THF solution, the guaiazulene complexes do not dissociate to the radical anions, which is indicated by the absence of ESR signals. Therefore, in the case of complex 1, the *ansa*-metallocene form reacts with Me_3SiCl instead of the ion form as in the case of the acenaphthylene derivatives. The ace-

naphthylene complexes dissociate readily to the radical anions likely due to the rather high thermodynamic stability of the acenaphthylene dianions formed at the second step. The reaction of the latter with Me_3SiCl affords 1,2-bis(trimethylsilyl)acenaphthylene and free acenaphthylene. The disproportionation of the guaiazulene radical anions in a solution to the dianion and neutral ligand is not thermodynamically favorable (because of the great difference in the first and second reduction potentials), which results, in fact, in the complete shift of equilibrium in the radical anions—metallocene system toward the latter.²¹

In this work, we presented new data that confirmed our primary idea that the radical anions of nonalternant hydrocarbons can recombine diastereoselectively to form *ansa*-metallocenes. Continuing our studies, we are planning to study the formation of *ansa*-metallocenes using metals with both larger (Sr, Ba) and smaller ion radii (Mg, Zn) than those of Ca and Yb.

Experimental

All procedures were carried out *in vacuo* or under dry nitrogen using the Schlenk techniques. Iodides $M_2(\text{THF})_2$ ($M = \text{Yb, Ca}$) were synthesized by the reactions of the corresponding metals with CH_2I_2 in THF. Tetrahydrofuran and 1,2-dimethoxyethane were dried, stored over sodium benzophenone ketyl, and sampled for reactions using condensation *in vacuo* prior to use. Guaiazulene was purchased from Aldrich. Suspensions of the complexes in Nujol were prepared to record IR spectra. IR spectra were obtained on a Specord M-80 spectrometer. NMR spectra were recorded on Bruker DPX-200 and Bruker ARX-400 instruments at $\sim 20^\circ\text{C}$. Chemical shifts are presented in ppm and compared with the chemical shifts of the residual protons and ^{13}C isotopes of deuterated solvents.

8,8'-Bis(1,4-dimethyl-7-isopropylazulenide)calcium tetrahydrofuranate (1). A mixture of $\text{CaI}_2(\text{THF})_2$ (4.95 g, 10.6 mmol), potassium (0.882 g, 22.6 mmol), and guaiazulene (4.48 g, 22.6 mmol) was magnetically stirred for 5 h in THF (40 mL) at 60°C . The mixture was left without stirring for 3 days, and KI was filtered off. Crystallized complex **1** was extracted with THF. The solvent was removed *in vacuo* from the extract, and a residue was washed with Et_2O (2×20 mL). After the residue was recrystallized from THF, compound **1** was obtained as large colorless crystals in 66% yield (4.37 g), m.p. 265°C (decomp.). Found (%): C, 78.66; H, 8.84. $\text{C}_{38}\text{H}_{52}\text{CaO}_2$. Calculated (%): C, 78.57; H, 9.02. ^1H NMR (200 MHz, THF- d_8), δ : 0.80 (d, 6 H, C(10)Me); 1.07 (d, 6 H, C(9)Me); 2.04 (s, 6 H, C(1)Me); 2.20 (s, 6 H, C(4)Me); 2.58 (m, 2 H, H(7), $J = 6.8$ Hz); 4.20 (s, 2 H, H(8)); 5.64 (d, 2 H, H(2), $J = 3.4$ Hz); 5.70 (d, 2 H, H(3), $J = 3.4$ Hz); 5.76 (d, 2 H, H(5), $J = 6.8$ Hz); 5.85 (d, 2 H, H(6), $J = 6.8$ Hz). ^{13}C NMR (50 MHz, THF- d_8), δ : 149.7, 134.7, 123.7, 122.4, 117.8, 117.3, 111.7, 110.1, 102.8, 44.8, 37.9, 24.4, 24.3, 21.6, 12.5. IR, ν/cm^{-1} : 1620 w, 1500 w, 1300 s, 1230 s, 1170 m, 1030 w, 970 s, 830 vs, 780 w, 745 m, 695 w, 665 w, 615 w, 545 w.

8,8'-Bis(1,4-dimethyl-7-isopropylazulenide)ytterbium tetrahydrofuranate (2a). A solution of guaiazulene (2.5 g, 6.3 mmol) in THF (10 mL) was added with vigorous stirring to a suspension of ytterbium naphthalenide $\text{C}_{10}\text{H}_8\text{Yb}(\text{THF})_2$ (2.8 g, 6.3 mmol) in THF (35 mL). A black powder of $\text{C}_{10}\text{H}_8\text{Yb}(\text{THF})_2$ was dissolved, and the mixture rapidly became red-brown. The reaction mixture was centrifuged and decanted from a small amount of a precipitate. The solution was concentrated to 10 mL by the removal of the solvent *in vacuo*. A sealed ampule containing the concentrated solution was placed in an refrigerator (-5°C). After 10 days, the solution was decanted from precipitated crystals, which were recrystallized from THF. Compound **2a** as large dark red lamellar crystals was obtained in 76% yield (3.75 g), m.p. $>200^\circ\text{C}$ (decomp.). Found (%): Yb, 22.37. $\text{C}_{38}\text{H}_{52}\text{O}_2\text{Yb} \cdot \text{C}_4\text{H}_8\text{O}$. Calculated (%): Yb, 22.01. ^1H NMR (200 MHz, THF- d_8), δ : 0.85, 0.98 (both d, 6 H each, Me, $J = 6.8$ Hz); 1.52 (m, 12 H, THF); 1.96, 2.13 (both s, 6 H each, Me); 2.47 (sept, 2 H, $J = 6.8$ Hz); 3.58 (m, 12 H, THF); 4.19 (s, 2 H); 5.30–5.60 (m, 6 H); 5.73 (d, 2 H, $J = 6.6$ Hz).

8,8'-Bis(1,4-dimethyl-7-isopropylazulenide)ytterbium pyridinate (2b). Prismatic black crystals of **2b** were obtained by the recrystallization of compound **2a** from Py, m.p. $>200^\circ\text{C}$ (decomp.). Found (%): Yb, 20.58. $\text{C}_{40}\text{H}_{46}\text{N}_2\text{Yb} \cdot \text{C}_5\text{H}_5\text{N}$. Calculated (%): Yb, 21.44. ^1H NMR (200 MHz, Py- d_5), δ : 1.09, 1.17 (both d, 6 H each, Me, $J = 6.5$ Hz); 1.52 (m, 12 H, THF); 2.10, 2.39 (both s, 6 H each, Me); 2.79 (m, 2 H, $J = 6.5$ Hz);

3.58 (m, 12 H, THF); 4.67 (s, 2 H); 5.77 (d, 2 H, $J = 2.7$ Hz); 5.88 (d, 2 H, $J = 6.6$ Hz); 5.97 (d, 2 H, $J = 2.7$ Hz); 6.10 (d, 2 H, $J = 6.6$ Hz).

8,8'-Bis(1,4-dimethyl-3-trimethylsilyl-7-isopropylazulene)

(3). A mixture of compound **1** (3.0 g, 5.17 mmol) and Me_3SiCl (2.1 g, 19.33 mmol) in THF (20 mL) was stirred for 5–10 min at 50°C . The solvent was removed *in vacuo*, and a residue was extracted with Et_2O . After the solvent was removed from the extract, compound **3** was obtained as colorless needle-like crystals in 92% yield (2.6 g), m.p. 168 – 170°C . Found (%): C, 79.15; H, 10.45. $\text{C}_{36}\text{H}_{54}\text{Si}_2$. Calculated (%): C, 79.63; H, 10.02. ^1H NMR (200 MHz, C_6D_6), δ : –0.22 (s, 18 H, Me_3Si); 0.76, 1.01 (both d, 6 H each, Me, $J = 6.0$ Hz); 1.52 (s, 6 H, $\text{Me}(1)$); 2.15 (s, 6 H, $\text{Me}(4)$); 2.33 (m, 2 H, H(8), $J = 6.0$ Hz); 3.44 (s, 2 H, H(3)); 3.61 (s, 2 H, H(10)); 5.69 (d, 2 H, H(6), $J = 6.0$ Hz); 5.96 (s, 2 H, H(2)); 6.19 (d, 2 H, H(5), $J = 6.0$ Hz). IR, ν/cm^{-1} : 1620 w, 1500 w, 1300 w, 1230 s, 1170 m, 1030 w, 970 s, 830 vs, 780 w, 745 m, 695 w, 665 w, 615 w, 545 w.

X-ray diffraction study of complexes 1, 2a, and 2b. Diffraction data for crystals of **1**, **2a**, and **2b** were obtained with a Siemens SMART CCD diffractometer (ω scan mode, Mo-K α radiation, $\lambda = 0.71073$ \AA , graphite monochromator) at 173°C . The SADABS program²² was used to apply corrections to absorption. The structures were solved by the direct methods using the SHELXS-97 program²³ followed by refinement using the full-matrix least-squares method against F^2 using the SHELXL-97 program.²⁴ All nonhydrogen atoms were refined in the anisotropic approximation. Hydrogen atoms were placed in the idealized positions ($U_{\text{iso}} = 0.08$ \AA^3). The PLATON program was used²⁵ for analysis of the geometric parameters of the structures of the complexes. The crystallographic data, parameters of X-ray diffraction parameters, and refinement parameters for complexes **1**, **2a**, and **2b** are presented in Table 1. The coordinates of atoms were deposited with the Cambridge Structural Data Base. The main bond lengths in molecules **1**, **2a**, and **2b** are given in Table 2.

This work was financially supported by the Russian Foundation for Basic Research (Project Nos. 01-03-32631 and 00-03-40116) and the Alexander von Humboldt Stiftung, FRG.

References

- I. L. Fedushkin, S. Dechert, and H. Schumann, *Angew. Chem., Int. Ed. Engl.*, 2001, **40**, 561.
- I. L. Fedushkin, T. V. Petrovskaya, M. N. Bochkarev, S. Dechert, and H. Schumann, *Angew. Chem., Int. Ed.*, 2001, **40**, 2474.
- I. L. Fedushkin, Yu. A. Kurskii, V. I. Nevodchikov, M. N. Bochkarev, S. Mühle, and H. Schumann, *Izv. Akad. Nauk, Ser. Khim.*, 2002, **151** [*Russ. Chem. Bull., Int. Ed.*, 2002, **51**, 160].
- P.-J. Sinnema, B. Twamley, and P. J. Shapiro, *Acta Crystallogr., Sect. E*, 2001, 438.
- I. L. Fedushkin, M. N. Bochkarev, S. Dechert, and H. Schumann, *Chem.-Eur. J.*, 2001, **7**, 3558.
- (a) A. Recknagel and F. T. Edelmann, *Angew. Chem., Int. Ed. Engl.*, 1991, **30**, 693; (b) M. Rieckhoff, U. Pieper,

D. Stalke, and F. T. Edelmann, *Angew. Chem., Int. Ed. Engl.*, 1993, **32**, 1079; (c) K. M. Kane, P. J. Shapiro, A. Vij, and R. Cubbon, *Organometallics*, 1997, **16**, 4567; (d) P. J. Shapiro, K. M. Kane, A. Vij, D. Stelck, G. J. Matare, R. L. Hubbard, and B. Caron, *Organometallics*, 1999, **18**, 3468; (e) J. J. Eisch, Xian Shi, and F. A. Owuor, *Organometallics*, 1998, **17**, 5219; (f) M. Könemann, G. Erker, R. Fröhlich, and S. Kotila, *Organometallics*, 1997, **16**, 2900.

7. F. A. Cotton, B. E. Hanson, J. R. Kolb, P. Lahuerta, G. G. Stanley, B. R. Stults, and A. J. White, *J. Am. Chem. Soc.*, 1977, **99**, 3673.

8. M. R. Churchill and P. H. Bird, *Inorg. Chem.*, 1969, **8**, 1941.

9. F. A. Cotton, B. E. Hanson, J. R. Kolb, and P. Lahuerta, *Inorg. Chem.*, 1977, **16**, 89.

10. H. Nagashima, A. Suzuki, M. Nobata, K. Aoki, and K. Itoh, *Bull. Chem. Soc. Jpn.*, 1998, **71**, 2441.

11. Ch. Elschenbroich and A. Salzer, *Organometallics. A Concise Introduction*, VCH Publishers, New York, 1989.

12. P. Burger, H.-U. Hund, K. Evertz, and H. H. Brintzinger, *J. Organomet. Chem.*, 1989, **378**, 153.

13. H. Schwemlein and H. H. Brintzinger, *J. Organomet. Chem.*, 1983, **254**, 69.

14. G. J. Matare, K. M. Kane, P. J. Shapiro, and A. Vij, *J. Chem. Crystallogr.*, 1998, **28**, 731.

15. B. Twamley, G. J. Matare, P. J. Shapiro, and A. Vij, *Acta Crystallogr.*, 2001, **57E**, m402.

16. P.-J. Sinnema, B. Twamley, and P. J. Shapiro, *Acta Cryst.*, 2001, **57E**, m438.

17. P.-J. Sinnema, B. Hoehn, R. L. Hubbard, P. J. Shapiro, B. Twamley, A. Blumenfeld, and A. Vij, *Organometallics*, 2002, **21**, 182.

18. A. T. Gilbert, B. L. Davis, T. J. Emge, and R. D. Broene, *Organometallics*, 1999, **18**, 2125.

19. A. V. Khvostov, B. M. Bulychev, V. K. Belsky, and A. I. Sizov, *J. Organomet. Chem.*, 1999, **584**, 164.

20. E. de Boer, *Adv. Organomet. Chem.*, 1964, **2**, 115.

21. H. Bock, C. Arad, Ch. Näther, and I. Göbel, *Helv. Chim. Acta*, 1996, **79**, 92.

22. G. M. Sheldrick, *Empirical Absorption Correction Program*, Universität Göttingen, Göttingen, 1996.

23. G. M. Sheldrick, *Program for Crystal Structure Solution*, Universität Göttingen, Göttingen, 1990.

24. G. M. Sheldrick, *Program for Crystal Structure Refinement*, Universität Göttingen, Göttingen, 1997.

25. A. L. Spek, *Acta Crystallogr.*, 1990, **46A**, 34.

*Received October 22, 2002,
in revised form February 25, 2003*